Universal molecule injector in liquid helium: Pulsed cryogenic doped helium droplet source

V. Ghazarian, J. Eloranta, and V. A. Apkarian[a)]
Department of Chemistry, University of California, Irvine, California 92697

(Received 17 May 2002; accepted for publication 10 June 2002)

Progress toward the construction of a universal molecule injector for doping bulk liquid helium is reported. A pulsed valve that operates at cryogenic temperatures, down to 4 K, is demonstrated within the confinement of a cryostat, operating in the vapor above a steady level of liquid He. The insulated valve can be operated at elevated temperatures with preseeded helium gas in supersonic expansion mode, as demonstrated through laser-induced fluorescence spectra of seeded NO_2. At cryogenic operating temperatures, the expansion into vapor helium produces a well-collimated liquid helium droplet beam, which is then used to transfer to the liquid impurities produced by laser ablation from a cryogenic rotating target. The operation can be visualized using copper as the ablation target: the droplet beam is imaged via Rayleigh scattering, while the beam past the plasma is imaged by the fluorescence of the entrained Cu atoms. The beam drags along copper ions and electrons, the recombination of which controls the fluorescence yield downstream. © *2002 American Institute of Physics.* [DOI: 10.1063/1.1505662]

I. INTRODUCTION

Investigations of spectroscopy, chemistry, and dynamics of molecular species in superfluid helium are the subjects of intense research at present.[1–5] Much of this progress has occurred by the cluster pickup technique, which was pioneered by Scoles,[6] and extensively developed by the Toennies[2] group among others.[7,8] Rather thorough reviews of the experimental and theoretical aspects of molecular studies in doped liquid droplets have appeared.[2,3] Beside the investigation of implications of superfluidity on microscopic scales,[9] these experiments have been used to take advantage of various properties of the droplets. For example, the very cold and inert nature of the clusters allows the isolation of delicately metastable species for spectroscopic investigations;[10] and the superthermal conductivity of the droplets coupled with mobility of species allows for unusual chemistry.[7] Despite the exciting advances made by the cluster technique, there are important reasons to consider the spectroscopy of molecules in bulk helium.[11] The limitation of thermodynamic variables in clusters, boundary effects due to finite size, inhomogeneities due to the large dispersion of cluster sizes, are among the reasons. Several techniques have been developed for the injection of atomic impurities in bulk helium.[1] The electrostatically driven injection of ions,[12] injection of ions with subsequent neutralization,[13] and *in situ* laser ablation,[14,15] direct coupling of discharged gas flow to the liquid,[16] are examples. These methods have succeeded mainly in the injection of atomic species. There does not yet exist a reliable method for injecting molecular species in liquid helium, under conditions suitable for spectroscopic studies—sufficient residence time and concentration.[17] This is the motivation behind the instrumental development that we present here. Our intention is to develop a sufficiently flexible molecule injector to be able to investigate stable and transient molecules in bulk He II (liquid helium below the λ point transition, which occurs at 2.17 K).[18] Beside the investigation of molecular dynamics in this unusual bath, ultimately we would like the capability to harness the products of expected unusual chemistry in measurable quantities. Our progress toward this aim has already produced valuable instrumental developments, such as the intense, pulsed, cryogenic droplet source, which we describe here; and which has already been used to advantage in cluster applications as described in the accompanying article by the Vilesov and Momose groups.[19]

A. Design considerations

Due to its self-purifying nature, He II is one of the purest condensates. In essence, bulk liquid helium may be regarded as the poorest of solvents. Accordingly, any doping of the fluid will be transient in nature. Through proper design, we can only hope to maximize the length of time between injection and phase separation of the dopant from the fluid. Also, to be able to take advantage of the properties of the bath, the doping must be accomplished under gentle enough conditions to ensure thermal equilibrium between impurity and fluid during the transient time of mixing. The high thermal conductivity of He II is to be relied on for this purpose.[18] Nevertheless, it is necessary to minimize the thermal load on the liquid—the injection process must be designed to precool internal degrees of freedom of the impurity and to reduce all latent heats of fusion. These considerations have dictated the design of our injector. The concept is to encapsulate molecular species first in large helium droplets, then to allow the doped droplets to softly land on the surface of the liquid. Since it is known that droplets pick up virtually any impurity that they encounter, even if some open shell species remain

[a)]Author to whom correspondence should be addressed; electronic mail: aapkaria@uci.edu

on the droplet surface, the presolvation concept can be expected to be universal. To guarantee soft landing of the doped droplets in the liquid, it is necessary to reduce the plug velocity of the droplet beam, which is determined by the source temperature.[20] Clearly, a nozzle that could operate at temperatures close to that of the liquid would be desirable. The practical design would dictate operation of a source at $T \sim 4.2$ K, maintained at that temperature by the vapor above the fluid. Finally, since we expect phase segregation of excess dopants, it is useful to inject the impurities at high densities only when needed. This calls for a pulsed injector, operating with a duty cycle matched to the spectroscopic measurements. In addition to increasing signal-to-noise ratio in spectroscopic measurements that use pulsed lasers, such a source would minimize heat and gas loads. The latter consideration is crucial to maintain a clear liquid–gas interface by minimizing the total amount of impurities injected during an experiment. Experience with continuous flow sources shows that with time, impurities freeze out as a film on the liquid surface. Indeed, we expect most measurements in the liquid phase to be carried out near the surface, before the dopants have a chance to cluster through diffusion controlled encounters. Quite clearly, if the nozzle operates at cryogenic temperatures, then it cannot be preseeded (except for ^{3}He and H_2). This dictates that impurities be picked up downstream. We use laser ablation as a general approach for producing the species to be crossed with the droplet beam. To this end we incorporate a rotating target as a laser ablation platform, using a motor that operates at the cryogenic temperatures maintained by the evaporating helium. Given the significant development in laser ablation science, knowledge exists for volatilizing nearly any desired molecular species.[21] Thus, the coupling of the cryogenic pulsed nozzle with the cryogenic laser ablation target over liquid helium contains all of the design elements of a universal molecule injector. Below, we describe the construction details and demonstration of the performance of the system.

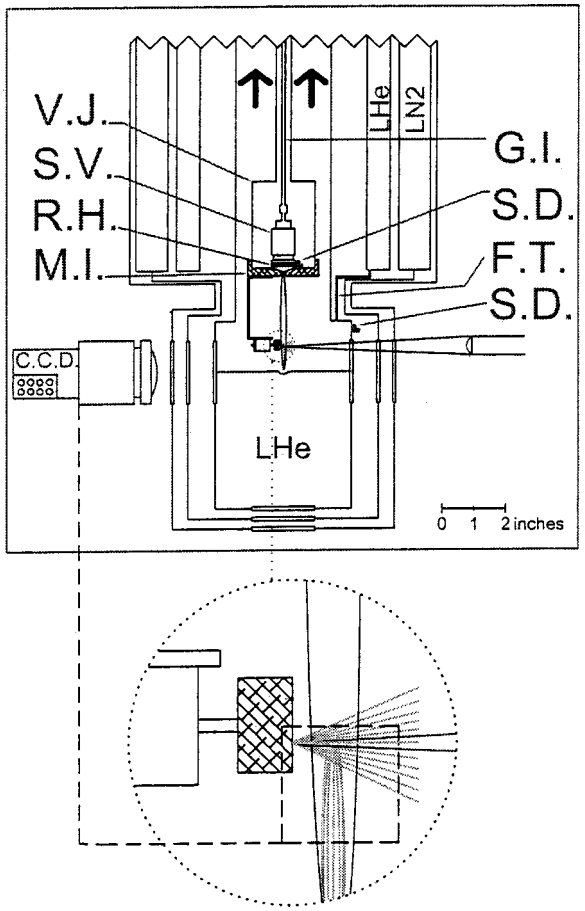

FIG. 1. Schematic of the cryostat, nozzle, and rotary ablation target: (V. J.) vacuum jacket around the valve; (S. V.) solenoid valve; (R. H.) resistive heater; (M. I.) macor insulating disk attached to the valve and jacket through indium seals; (S. D.) silicon diode temperature sensors; (F. T.) fill tube for the liquid helium; (G. I.) gas inlet made of 1/8 in. ss tubing; and (C. C. D.) imaging color camera. The ablation laser, rotating target, He beam, and liquid helium with a dimple on the surface are shown schematically. The drawing is to scale except for the section showing the liquid He and liquid N_2 reservoirs. In the expansion below, with the dashed square, we show the area imaged by the camera, which is displayed in Figs. 3, 4, and 6.

II. EXPERIMENTAL APPARATUS

A. Cryostat

The experiments are carried out in a custom designed, optical helium cryostat (Oxford). The inner copper shaft of the cryostat, where the liquid is held, has a diameter of 7.5 cm. The liquid hold can be accessed through five sets of optical windows, three windows in each set, as illustrated in Fig. 1. Liquid helium is delivered from a 15 L reservoir, a capacity sufficient for 50 h of continuous operation in the absence of thermal loads. The temperature of the liquid is controlled to ± 0.05 K through resistive heating under a proportional integral differential control (Lakeshore Model 321) and by manual control of the helium flow rate. Temperature is monitored through a pair of calibrated silicon diodes. The liquid is pumped with a 35 cubic feet per minute (CFM) trapped mechanical pump, which is throttled to maintain steady evaporation at the saturated vapor pressure of the liquid $P = 0.3–30$ Torr. The radiative heat flux through the optical windows limits the achievable base temperature to 1.45 K. Heat load management is the critical consideration in the design of the various inserts in order to provide a stable liquid level during measurements.

B. Pulsed cryo-valve

A commercial solenoid valve (Parker Hannifin, General Valve, Series 99), with spring loaded action in both open and close strokes, and 0.2 mm orifice, is used to generate a directed beam. The valve generates a pulsed supersonic expansion when operating at high temperatures, and a liquid helium droplet beam when cooled. With some care to details of assembly, the valve can be reliably operated at temperatures as low as 4.2 K, when bathed with liquid He. Under normal operating temperatures, poppets made of elastomers are used to form a tight seal through plastic deformation. Since the sought cryogenic temperature of operation is below the glass transition of elastomers, the seal now must be made by maintaining tight tolerances between hard surfaces. A polished surface on the poppet cone and a round valve seat with a sharp edge is necessary. Deformation or blemishes on either

surface, while forgiving at room temperature, lead to leaks at cryogenic temperatures. Inspection of the poppet and the valve seat under $\times 40$ magnification is usually sufficient to determine whether a valve will operate or fail under cryogenic conditions. We use Kel–F for the poppet material, and the bullet nose geometry for the tip.

The system was designed for two modes of operation:

(a) coupling a hot nozzle to the cold bath, using a preseeded supersonic expansion; and
(b) cryogenic operation of the valve to generate large helium droplets, to be seeded by laser ablation, and subsequent soft landing of the doped droplets.

In the first mode of operation, good insulation of the valve to minimize radiative and convective heat loads on the liquid is essential. The design that accomplishes this is shown in Fig. 1. The 1/8 in. stainless steel (ss) tubing that supplies the gas to the valve is wrapped in layers of silvered mylar, and is contained in a vacuum jacket. The connection between the valve and the polished ss jacket is made through a 1/4 in. thick macor disk, which is thinned into a cone at the center to avoid obstructing the gas expansion. The macor is sealed to the valve and vacuum jacket with indium gaskets. Multiple layers of silvered mylar sheets provide additional insulation in all critical interfaces. The pulsed valve is resistively heated. This design has enabled operation of the valve at a distance of 7 cm above the liquid, at a nozzle temperature of 170 K, while maintaining the liquid at $T=1.7$ K at an acceptable rate of evaporation. Under these conditions, at a backing pressure of 4 bar, for nominal pulse widths of <400 μs, the supersonic beam could be effectively coupled to the liquid. This is verified visually, by observing the formation of a stationary dimple at the liquid surface where the beam is delivered. The opening time of the valve is adjusted to prevent liquid from splattering.

In the cryogenic operation mode, the temperature of the nozzle and the backing pressure of the gas can be adjusted to effect expansion either from the gas side or the liquid side of the helium phase diagram. When expanded in vacuum ($P<10^{-3}$ Torr), it is known that both of these approaches yield large helium clusters through mechanisms that have been characterized experimentally[22,23] and modeled theoretically.[24] In the first case, adiabatic cooling of the gas leads to clustering during the expansion with cluster sizes $N<10^4$, determined by the stagnation temperature and pressure. In the case of expansion from the liquid side, the droplets undergo evaporative cooling to shrink to a bimodal terminal size distribution, with the larger droplets containing $N>10^6$ atoms. These conditions are reached in the present design while operating as a cluster beam, in the absence of the liquid, as has been verified.[19] The operating conditions of our ultimate application are somewhat unusual, since the droplet beam must be expanded into the vapor above the liquid (saturated vapor pressure ranging from 0.3 to 30 Torr). Moreover, to achieve conditions of ''soft landing,'' it is desirable to operate the nozzle at the lowest possible temperature. Although the valve operates reliably at 4 K, and assembly need not be adjusted for repeated heating/cooling cycles, its operating characteristics change with temperature. The performance of the expansion under different stagnation pressure and temperature conditions, and as a function of temperature and pressure in the expansion chamber, are directly visualized using a color charge coupled device (CCD) camera (Sony DXC-390). The beam is imaged by the Rayleigh scattered light from the ultraviolet (UV) ablation laser, while the beam downstream from the ablation site is imaged by recording the fluorescence of the entrained, ablated species (see below). Note, since the nozzle is cooled by the cold He vapor, its insulation presents the disadvantage of inefficient cooling. At a repetition rate of 10 Hz, the nozzle temperature climbs up from the ambient of 4 K to 15 K due to the heat dissipated in the solenoid. Thermal shorting, by filling the inner vacuum jacket with helium gas allows 10 Hz operation at a nozzle $T<10$ K, with the liquid maintained below the λ point.

C. Cryogenic, rotating ablation target

A hobby shop motor is used to rotate the ablation target at temperatures as low as 4 K. The motor is mounted on a bracket, fixed to the bottom of the valve assembly 5 cm below the nozzle (see Fig. 1). Its placement is optimized for efficient coupling between the ablation plume and beam, without destroying the beam expansion profile. These adjustments are made using the CCD camera, which is mounted behind a macro lens with adjustable magnification. Cooling reduces the resistance of the windings of the motor, and increases the current demand for steady rotation (typical operating power is 100 mW). Also, step rotation could be achieved with a function generator, in which case the consumed rms power is reduced to ~10 mW. The associated heat load on the liquid is tolerable, as judged by the rate of evaporation. Rather stable ablation is also possible for extended periods from stationary targets.

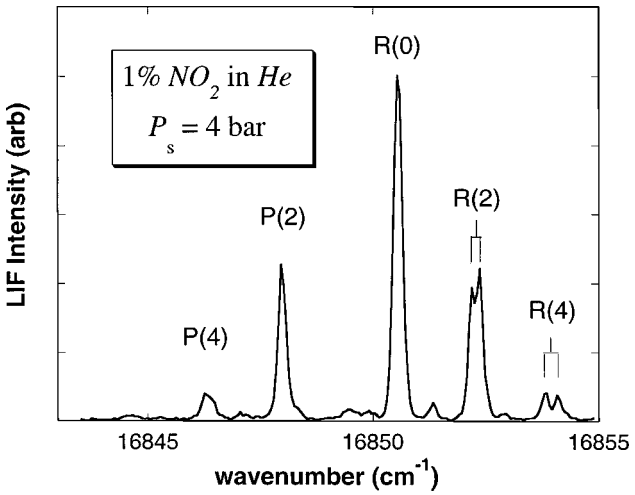

FIG. 2. Excitation spectrum of NO_2 in the supersonic expansion from the room temperature nozzle. The example is from a 1% mixture of NO_2 in He, expanded at stagnation pressure of 4 bar. The observable splitting of the $R(2)$ and $R(4)$ lines is due to spin-rotation coupling (see Ref. 25). The relative intensity of the $R(0)$ to $P(2)$ line is used to extract a rotational temperature of $T=1.6$ K.

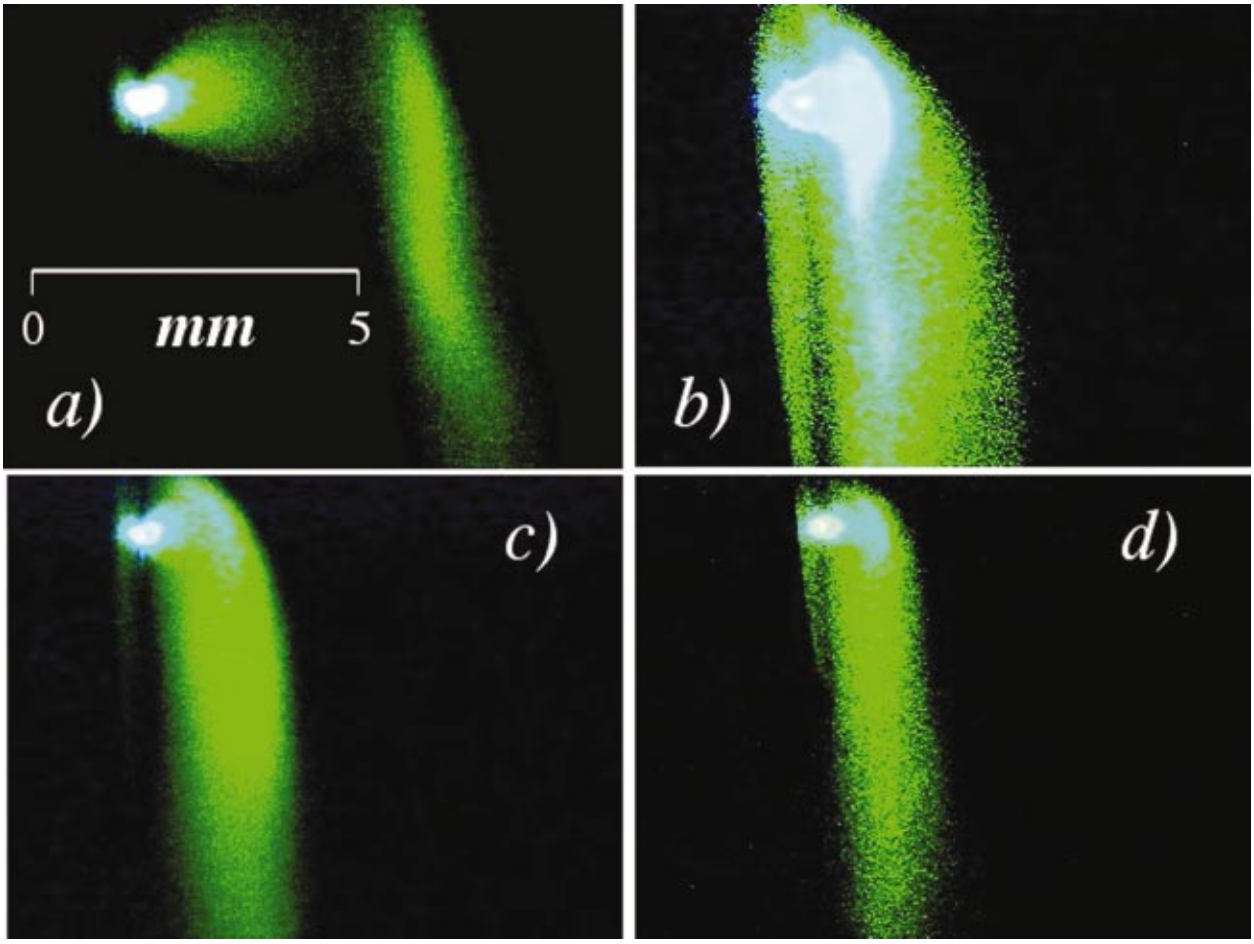

FIG. 3. (Color) Room temperature operation of the nozzle in supersonic expansion mode, and pickup of laser ablated copper atoms (for the field of view of the camera, see bottom part of Fig. 1). (a) Laser ablated Cu plume in vacuum, with misaligned gaseous helium beam. (b) Attachment of the plasma to the gaseous beam is indicated by the distorted white core (stagnation pressure = 5 bar, chamber pressure = 20 Torr). (c) Beam expanded with a stagnation pressure of 5 bar, into chamber at a pressure of 9 Torr. (d) Expansion at a stagnation pressure of 4 bar, into chamber at a pressure of 14 Torr. Note, in all cases the image to the left of the plasma is a reflection off the ablation target, which is a polished copper disk. The indicated scale applies for (a), (c) and (d), the image in (b) is further magnified by 50%.

In the present setup, with pulsed valve and rotating ablation target operating near 10 K, 5 cm above the liquid level, the liquid could be maintained below the λ point.

III. PERFORMANCE

A. Operation in supersonic expansion mode-warm nozzle

Given the confined environment of the nozzle and the relatively low pumping speed used, it is important to test whether the required expansion ratios can be reached for generating a supersonic beam.[20] This we test by expanding helium seeded with 1% NO_2, by recording the well-known excitation spectrum of this molecule,[25] using laser induced fluorescence (LIF) for detection. A typical spectrum is shown in Fig. 2. From the intensity ratio between the $P(2)$ and $R(0)$ lines of 0.5, using the spacing between these lines of $6\ B = 2.4\ cm^{-1}$, the rotational temperature of NO_2 can be established as 1.6 K. Clearly, the arrangement allows efficient cooling through supersonic expansion. The operation of the expansion was tested as a function of backing pressure, and as a function of pressure in the expansion chamber. The latter was intended to simulate conditions of operation when the beam is coupled to the liquid. Expansion into a background pressure of 1 Torr at a backing pressure of 10 bar, produced comparable rotational cooling in NO_2. Despite the low temperature of the molecule, the spectra do not contain any evidence of clustered species. This, we take as an indication that the monitored fluorescence of NO_2 is quenched by helium; and we conclude that LIF of NO_2 is unsuitable for detecting molecules in the liquid phase.

B. Laser ablation seeding and imaging of the pulsed beam

The use of a rotating copper disk provides a convenient target for ablation, with the additional benefit that the characteristic copper fluorescence plume ($4\,^2P_{3/2} \rightarrow 5\,^2D_{5/2}$ transition at 510.6 nm, with radiative lifetime $\tau = 0.5\ \mu s$) allows visualization of the beam and the pickup process. Either a XeCl excimer laser (308 nm, 40 mJ/pulse, 15 ns pulse width), or the tripled output of a yttrium–aluminum–garnet laser (355 nm, 7 mJ/pulse, 4 ns pulse width) was used as the ablation source. A single lens (focal length. = 20 cm) was used for focusing. Fluorescence at 90° was collected, dispersed through a 1/4-meter monochromator, and detected using a CCD array to identify the emission lines.

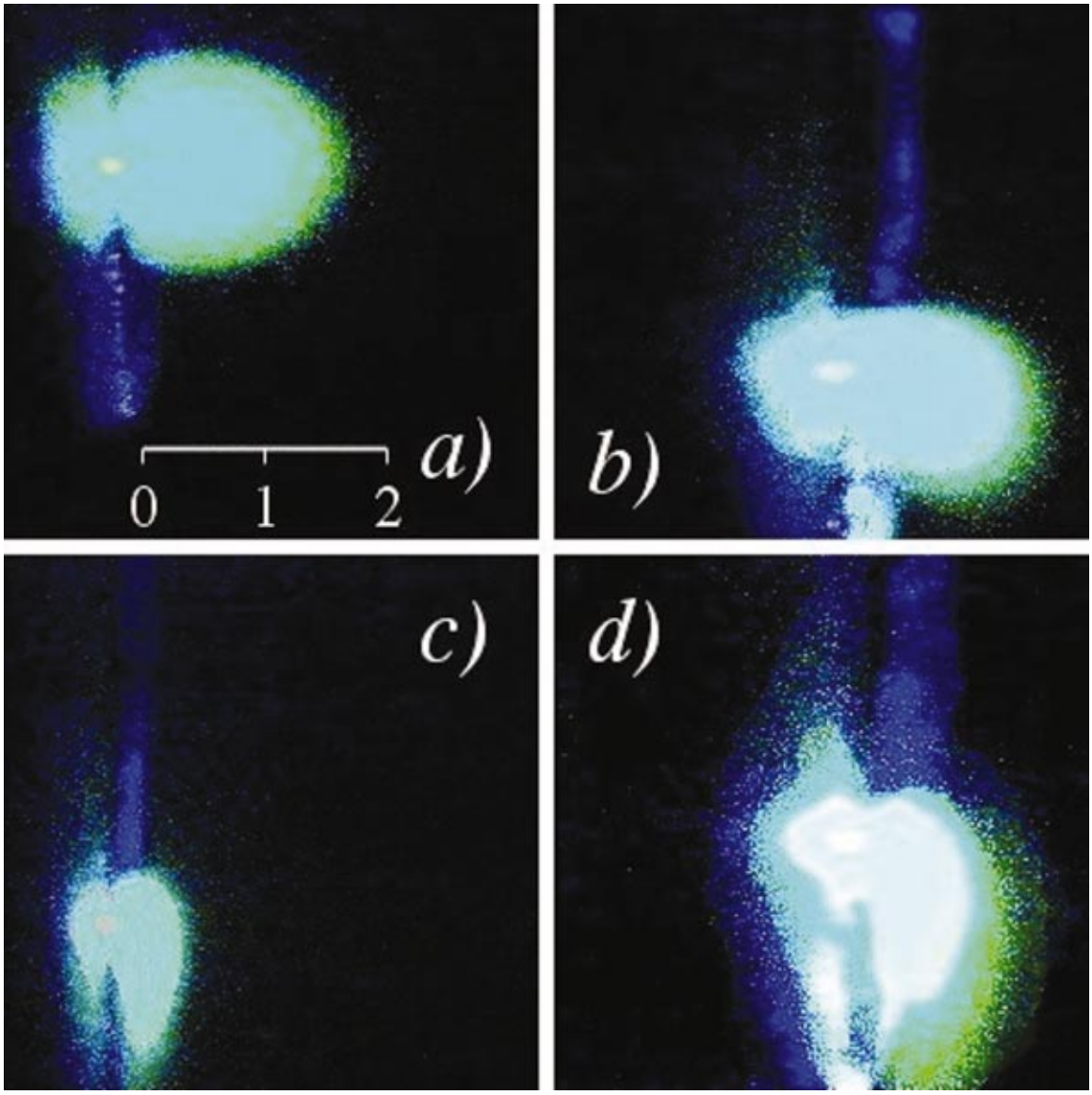

FIG. 4. (Color) Droplet beam and its traversal through the ablation zone, with nozzle at $T=50$ K, and chamber at $P=30$ Torr. The images are snapshots at different delays between valve and laser trigger (for the field of view of the camera, see bottom part of Fig. 1) (a) Ablation with beam off. The contour of the lower part of the copper disk (9 mm diameter) appears as a dark blue ellipse below the ablation spot, via scattering of the UV laser (308 nm). (b) Droplet beam observable above plasma through Rayleigh scattering of the ablation laser. The droplet beam has just reached the plasma, as evidenced by the small distortion of the plume. (c), (d) Successive larger distortions of the plasma by the piercing droplet beam. The scale shown applies for (a) and (c), while (b) and (d) are further magnified by a factor of 2. In all cases, the images to the left of the plasma core are reflections from the polished copper disk.

In Fig. 3, we illustrate the process for the supersonic expansion from the room temperature nozzle. When the ablation is carried out in vacuum, the green plume extends ~0.25 cm beyond the plasma which appears as a bright white core. This can be seen in Fig. 3(a), which also shows the misaligned molecular beam, as it sweeps the fluorescing Cu atoms downstream. The observation of a dark region between the plume and the beam is informative. As the plasma rarefies, the fluorescence subsides. This explains the dark region following the plume as it expands in vacuum. The subsequent resumption of intense fluorescence from the denser helium beam volume suggests that the atomic emission is the result of recombination between ions and electrons. Multiple scattering in the helium beam effectively cools the charged particles, and their recombination rate is greatly enhanced by the presence of a third body. The coupling of the plasma to the beam can be observed in Fig. 3(b), in which the beam is properly aligned, and the bright plasma core is strongly distorted downward. The images are limited to ~0.6 cm by the field of view of the camera, however, the fluorescence which traces the beam path remains visible for a distance of ~10 cm. This length scale is consistent with the expectation that the electronically excited Cu atoms will be swept by the beam. Thus, given the plug velocity of the room temperature expansion of 1300 ms^{-1}, within the fluorescence lifetime of the Cu($4\,^2P_{3/2}$) atoms of $\tau=0.5$ μs, a fluorescent trail of 6.5 cm is to be expected. Indeed, while fluorescence from the plasma shows a large number of atomic and ionic lines, the downstream fluorescence only reveals the atomic $4\,^2P_{3/2}\rightarrow 5\,^2D_{5/2}$ transition.

As the ambient pressure in the expansion chamber is increased, both the ablation plume and the beam contract in

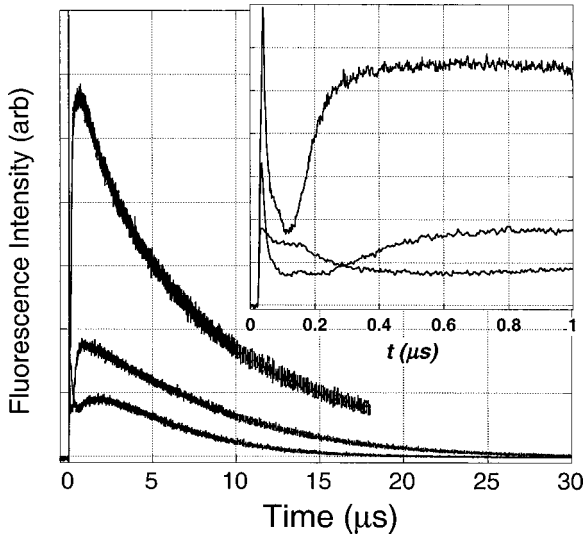

FIG. 5. Fluorescence time profile of Cu atoms (at 510 nm) entrained in the droplet beam. The data were recorded as a function of the pressure in the chamber, and the accompanying equilibrium temperature of the nozzle: (a) $P=5$ Torr, $T=27$ K; (b) $P=14$ Torr, $T=30$ K; and (c) $P=20$ Torr, $T=33$ K.

length. This is illustrated in Figs. 3(c) and 3(d), for expansions into 9 and 14 Torr of helium, respectively (backing pressure of 5 bar). As the chamber pressure is increased, the fluorescent trail shrinks in length and becomes narrower in width—from 3 mm at 9 Torr to 2 mm at 14 Torr. In effect, the ambient pressure acts as a skimmer. In the 5 cm travel from nozzle to ablation point the mach disk is destroyed, and only the collimated core survives. The reduction in the length of the fluorescent trail is to be expected as a consequence of the collision-induced reduction in plug velocity and length of directed flow.

Since the arrival of the beam to the ablation zone can be accurately determined through imaging, the performance of the valve and the beam under different conditions could be tested. When a 250-μs-long gate voltage is applied to the valve, the time duration for which the plasma distortion can be seen is 325 μs. This, we associate with the open period of the valve. It can be concluded that the room temperature response time of the solenoid action is 75 μs, implying that 150 μs is the minimum gate for complete opening. At settings below 50 μs, the valve does not open at all, as verified by the absence of any pressure rise in the chamber. These parameters may vary based on assembly of the valve, and its operating *P, T* conditions.

C. Cryogenic operation

As the temperature of the nozzle drops, the transition from gas beam to liquid droplet beam can be observed by the sudden enhancement of Rayleigh scattering from the droplets. This is illustrated in Fig. 4, for a nozzle temperature of 50 K and a stagnation pressure of 5 bar. In Fig. 4(a), the plasma is shown with the beam off, generated at a chamber pressure of 30 Torr. The copper plume is further contracted by collisions with the cold gas, limiting the atomic fluorescence to a thin green halo of ~0.025 cm around the cosine distribution of the plasma. In Fig. 4(b), the Rayleigh scattered radiation from the ablation laser (308 nm) can be seen as a blue beam above the slightly distorted plasma. The droplet beam is now significantly tighter, with a width of 0.5 mm. Recognizing that the nozzle orifice is 0.2 mm, and that the measurement is made 5 cm downstream from the orifice, it becomes apparent that the performance is more typical of a skimmed beam.[20] The increasing distortion of the plasma due to coupling to the droplet beam can be seen in Fig. 4(b) and 4(c). In each of these images the beam can be seen both before and after crossing the plasma. Above the plasma it appears blue due to the scattered laser, while below the plasma, it appears green due to the copper fluorescence [the colors are determined by the red–blue–green response of the camera]. The notable finding is that a well-collimated, intense droplet beam is formed under the unusual conditions of expansion into a chamber filled with 30 Torr of helium vapor and a nozzle temperature of 50 K.

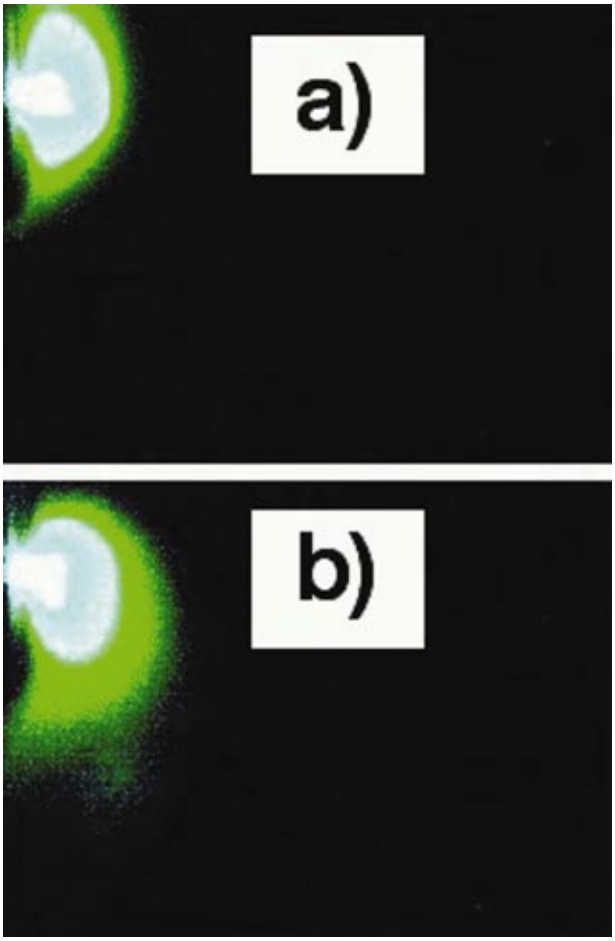

FIG. 6. (Color) Cryogenic expansion, with ablation target situated 2 cm above the liquid level (for the field of view of the camera, see bottom part of Fig. 1). (a) ablation with beam off and (b) ablation with beam on, nozzle temperature=15 K, chamber pressure=9 Torr, liquid temperature=2 K.

This finding is surprising especially in view of the results of Slipchenko *et al.*, who establish that when expanded in vacuum, a nozzle temperature of 50 K does not produce a detectable flux of liquid droplets.[19] Evidently, when operating over the cold vapor, droplet formation occurs by postexpansion condensation. This is a significantly different mecha-

nism of generating a collimated helium beam—a mechanism that is not well understood at present.

Cooling of the nozzle in our apparatus is provided by the cold helium vapor. As such, when cooling, there necessarily will be cold gas in the chamber. This alone leads to compression of the copper plume, as can be discerned in the comparison between Figs. 3(a) and 4(a). Also, as compared to the gaseous beam (Fig. 3), neutralization of the ions occurs on a much shorter length scale in the denser droplet beam [Fig. 4(c)]. Accordingly, only a very short length of ~1 mm of the trail can be imaged by the Cu fluorescence. This contraction of the trail can result from one of two possibilities: (a) the fluorescence is quenched in the droplet beam or (b) the plug velocity of the beam is now dramatically lower than that of the room temperature expansion. To distinguish between these two possibilities, we investigate the atomic fluorescence time profile. Data obtained at different chamber pressures, with concomitant variation in nozzle temperatures $T < 35$ K, are shown in Fig. 5. After the initial plasma spike, the fluorescence rises on the time scale of 0.5–1 μs, with delay increasing in proportion to the chamber pressure. The fluorescence then decays, nonexponentially, on the time scale of 5–10 μs. Clearly, the rise time is determined by the fluorescence lifetime while the decay represents the slower formation kinetics of the upper state, consistent with the neutralization mechanism, as already suggested above. While it is not clear whether excited atoms survive the pickup process, it is clear that the beam is rather efficient in picking up ions and electrons. It is valuable to note that positive ions serve as centers for condensation of helium, by forming snowballs.[1] As such, the plasma may further catalyze condensation, and the formation of larger droplets. This also implies that the droplet-solvated ions undergo recombination, a process that may release energy by evaporation. Quite clearly, the coupling of the droplet beam to the plasma will contain nontrivial microscopic dynamics, including the thermalization of fast electrons and the trapping and neutralization of ion–electron pairs. Finally, let us note that a measure of the plug velocity of the beam can be inferred from the observation that over its ~10 μs duration (Fig. 5), the fluorescent volume remains within ~1 mm [Figs. 4(c) and 4(d)], implying a velocity of ~100 m/s. This is significantly lower than what would be expected based on the nozzle temperature if the expansion was carried out in vacuum. For example, in their careful measurements, Slipchenko *et al.* find a beam velocity of 394 m/s for a nozzle temperature of 14 K. The significantly reduced beam velocity in the present arrangement again implies postexpansion cooling of the beam as it travels through the cold gas.

In Fig. 6 we show the plasma [Fig. 6(a)] and its attachment to the droplet beam [Fig. 6(b)], at a nozzle temperature of 15 K (during 10 Hz operation). These images were obtained with the level of the bulk He II only ~2 cm below the ablation spot. Although the fluorescence trail does not stretch far enough to reach the liquid, delivery to the bulk is easily identified by observing splashing at the surface. As in the case of the room temperature measurement, we monitor the length of time for which the plasma remains distorted. With the valve set for a nominal open time of 250 μs, we observe the distortion to last for as long as 4 ms (325 μs at room temperature). This implies that at the cryogenic temperatures of operation, with the chamber filled with cold He vapor, the beam stretches significantly beyond the valve opening time. We suspect that the droplets are segregated in size, with the heavier, colder droplets significantly trailing the warmer front with a velocity that is estimated to be $\leqslant$50 m/s; namely, below the Landau critical velocity required to generate elementary excitations in superfluid helium.[18] While we do not fully understand the dynamics of these droplet beams, it would seem that the conditions for ''soft landing'' are reached.

Operationally, all design considerations of the conceived molecule injector have been demonstrated. The next stage of this development will be the integration of a second laser, for interrogation of the injected impurities downstream from the ablation source, and after delivery to the liquid. The utility of the extant development as an intense, pulsed, doped, superfluid helium droplet source is addressed in the following article by Slipchenko *et al.*[19]

ACKNOWLEDGMENTS

This research was made possible through a grant from the U.S. AFOSR (Grant No. F49620-01-1-0449). Fellowships to J.E. from the Finnish Academy and to V.G. from GAANN are gratefully acknowledged. The authors also thank A. Vilesov *et al.* for delaying the publication of their manuscript until ours was completed, and for providing useful feedback from their experience. The contributions of R. Zadoyan, A. Boyamyan, M. Petterson, and the assistance of M. Karavitis, D. Segale, and M. Sgroi to various aspects of these experiments are gratefully acknowledged.

[1] B. Tabbert, H. Gunther, and G. zu Putlitz, J. Low Temp. Phys. **103**, 653 (1997).
[2] J. P. Toennies and A. F. Vilesov, Annu. Rev. Phys. Chem. **49**, 1 (1998).
[3] K. B. Whaley, in *Advances in Molecular Vibrations and Collision Dynamics*, edited by J. Bowman (JAI Press, Greenwich, CT, 1998), Vol. 3.
[4] J. P. Higgins, J. Reho, F. Stienkemeier, W. E. Ernst, K. K. Lehmann, and G. Scoles in *Atomic and Molecular Beams*, edited by R. Campange (Springer, Berlin, 2001).
[5] J. P. Toennies, A. F. Vilesov, and K. B. Whaley, Phys. Today **54**, 31 (2001).
[6] S. Goyal, D. L. Schutt, and G. Scoles, Phys. Rev. Lett. **69**, 933 (1992).
[7] K. Nauta and R. E. Miller, Science **283**, 1895 (1999); **287**, 293 (2000).
[8] T. Ruchti, K. Forde, B. E. Callicoatt, H. Ludwigs, and K. C. Janda, J. Chem. Phys. **109**, 10679 (1998).
[9] J. P. Toennies, *Advances in Quantum Many-Body Physics*, edited by E. Krotscheck and J. Navarro (World Scientific, Singapore, 2002), Vol. 4.
[10] J. Higgins, W. E. Ernst, C. Callegari, J. Reho, K. K. Lehmann, G. Scoles, and M. Gutowski, Science **273**, 629 (1996).
[11] A. Benderskii, J. Eloranta, and V. A. Apkarian, J. Chem. Phys. (in press).
[12] W. I. Glaberson and W. W. Johnson, J. Low Temp. Phys. **20**, 313 (1975); H. Bauer, M. Hausmann, R. Mayer, H. J. Reyher, E. Weber, and A. Winnacker, Phys. Lett. A **110**, 279 (1985).
[13] H. Bauer, M. Beau, A. Bernhardt, B. Freidl, and H. J. Reyher, Phys. Lett. A **137**, 217 (1989).
[14] T. Yabuzaki, A. Fujisaki, K. Sano, T. Kinoshita, and Y. Takahashi, in *Atomic Physics*, edited by H. Walther, T. W. Hansch, and B. Neizert (North Holland, New York 1992), Vol. 13, p. 337; Y. Takahashi, K. Sano, T. Kinoshita, and T. Yabuzaki, Phys. Rev. Lett. **71**, 1035 (1993).

[15] J. H. M. Beijersbetgen, Q. Hui, and M. Takami, Phys. Lett. A **181**, 393 (1993).
[16] E. B. Gordon, V. V. Khmelenko, A. A. Pelmenev, E. A. Popov, O. F. Pugachev, and A. A. Shestakov, Chem. Phys. **170**, 411 (1993).
[17] In our own experience of *in situ* laser ablation from molecular targets, such as from a rotating target of solid iodine, we have only succeeded in obtaining large clusters.
[18] J. Wilks and D. S. Betts, *An Introduction to Liquid Helium* (Oxford University Press, New York, 1987).
[19] M. N. Slipchenko, S. Kuma, T. Momose, and A. F. Vilesov, J. Chem. Phys. **117**, 1201 (2002).
[20] *Atomic and Molecular Beams*, edited by G. Scoles (Oxford University Press, New York, 1993).
[21] J. C. Miller, in *Laser Ablation: Principles and Applications*, edited by J. C. Miller (Springer, Berlin, 1994), p. 1.
[22] H. Buchenau, E. L. Knuth, J. Northby, J. P. Toennies, and C. Winkler, J. Chem. Phys. **92**, 6875 (1990).
[23] T. Jiang and J. A. Northby, Phys. Rev. Lett. **68**, 2620 (1992).
[24] D. M. Brink and S. Stringhari, Z. Phys. D: At., Mol. Clusters **15**, 257 (1990).
[25] R. E. Smally, L. Wharton, and D. H. Levy, J. Chem. Phys. **63**, 4977 (1975).